



Volume 127

2025

p-ISSN: 0209-3324

e-ISSN: 2450-1549

DOI: <https://doi.org/10.20858/sjsutst.2025.127.14>



Journal homepage: <http://sjsutst.polsl.pl>

Article citation information:

Rudzinskyi, V., Lomakin, V., Melnychuk, S., Yemets, B., Lyashuk, O., Ryabchuk, O., Slobodian, L. Chaotic behavior in the rotational speed of internal combustion engines. *Scientific Journal of Silesian University of Technology. Series Transport*. 2025, 127, 237-255. ISSN: 0209-3324. DOI: <https://doi.org/10.20858/sjsutst.2025.127.14>

**Volodymyr RUDZINSKYI¹, Volodymyr LOMAKIN², Serhii MELNYCHUK³,
Bogdan YEMETS⁴, Oleg LYASHUK⁵, Oleksandr RYABCHUK⁶,
Liubomyr SLOBODIAN⁷**

**CHAOTIC BEHAVIOR IN THE ROTATIONAL SPEED OF INTERNAL
COMBUSTION ENGINES**

Summary. This study investigates the chaotic behavior in the rotational speed of internal combustion engines. High-precision measurements of engine rotational speed were taken at discrete intervals of 0.36 degrees with time measured to a precision of 41 nanoseconds. The data was analyzed using various techniques from

¹ Department of Automobile Transport, Zhytomyr Agricultural Technical Professional College, Pokrovska Street 96, 10031 Zhytomyr, Ukraine. Email: vladimirrudzinskiy@bigmir.net.
ORCID: <https://orcid.org/0000-0002-0540-9740>

² Department of Automobile Transport, Zhytomyr Agricultural Technical Professional College, Pokrovska Street 96, 10031 Zhytomyr, Ukraine. Email: rootssymbol@gmail.com. ORCID: <https://orcid.org/0000-0002-8159-0166>

³ Department of Automobile Transport, Zhytomyr Agricultural Technical Professional College, Pokrovska Street 96, 10031 Zhytomyr, Ukraine. Email: sergij.m@ukr.net. ORCID: <https://orcid.org/0000-0001-6387-6489>

⁴ Department of Automobile Transport, Zhytomyr Agricultural Technical Professional College, Pokrovska Street 96, 10031 Zhytomyr, Ukraine. Email: bogdan1199@ukr.net. ORCID: <https://orcid.org/0000-0003-1015-8859>

⁵ Faculty of Engineering of Machines, Structures and Technologies, Ternopil Ivan Puluj National Technical University, Ruska 56 Street, 46000 Ternopil, Ukraine. Email: oleglashuk@ukr.net.
ORCID: <https://orcid.org/0000-0003-4881-8568>

⁶ General Technical Disciplines Department, Zhytomyr Agricultural Technical Professional College, Pokrovska Street 96, 10031 Zhytomyr, Ukraine. Email: nostradamus1969@ukr.net.
ORCID: <https://orcid.org/0009-0009-1154-3194>

⁷ Faculty of Engineering of Machines, Structures and Technologies, Ternopil Ivan Puluj National Technical University, Ruska 56 Street, 46000 Ternopil, Ukraine. Email: slobodyanlybchik48@gmail.com.
ORCID: <https://orcid.org/0000-0002-9191-6801>

chaos theory and nonlinear dynamics, including Lyapunov exponent calculations, phase space reconstruction, and power spectral density analysis. Results reveal that engine rotational speed exhibits complex, chaotic behavior across different operating conditions. Lyapunov exponents ranged from -0.004 to 0.024, indicating varying degrees of chaos from near-stability to strong chaotic behavior. The strongest chaos was observed at certain idle speeds, while full gas conditions showed milder but persistent chaotic characteristics. The study demonstrates that rotational speed fluctuations in internal combustion engines go beyond simple periodic or random variations, suggesting that traditional linear models may be insufficient for accurately predicting and controlling engine behavior. These findings have significant implications for engine design, control strategies, and diagnostics. The authors provide access to the original datasets and analysis code, encouraging further research and collaboration in this field. This work contributes to a deeper understanding of engine dynamics and may lead to the development of more sophisticated, nonlinear approaches to engine analysis and optimization.

Keywords: rotational speed, rotation per minute, chaos, chaotic distribution, internal combustion engine

1. INTRODUCTION

Chaos theory examines the intricate behavior of nonlinear dynamical systems, composed of interacting elements that collectively exhibit complex behavior. These systems are termed "nonlinear" because their interactions produce outcomes influenced by feedback and multiplicative effects, resulting in a whole greater than the sum of its parts. "Dynamical" indicates these systems evolve over time, with changes depending on their current state. Many real-world systems are nonlinear and dynamical in nature. Chaotic systems, a subset of these, can display complex and unpredictable behavior even with a small number of interacting components governed by simple rules. A defining feature of chaotic systems is their sensitivity to initial conditions, where minor differences at the start can lead to dramatically different outcomes over time. Contrary to expectations that simple deterministic systems would yield predictable behavior, chaotic systems can produce highly erratic and divergent patterns. These patterns often exhibit fractal characteristics, showing intricate and self-similar structures that never exactly repeat. The inherent sensitivity of chaotic systems means that long-term predictions are extremely difficult, as even the slightest measurement inaccuracies can result in vastly different future states. Chaos theory highlights the fundamental limits of predictability in certain systems and suggests that precise knowledge of future states is often unattainable. Furthermore, small interventions in chaotic systems can lead to unpredictable consequences, as tiny changes can be amplified or diminished in complex, nonlinear ways [1, 2].

Chaotic processes are prevalent, and chaos theory aids in predicting behavior across various fields. Unfortunately, such a background is not commonly applied in engineering practice. Internal combustion engines consist of numerous small, independent processes that can exhibit chaotic behavior. Nevertheless, the application of chaos theory to fundamental output data such as rotational speed or power is not widespread, though similar approaches exist in the literature, for example [2-6]. This study aims to demonstrate a chaotic approach for better understanding the behavior of the rotational speed of a four-cylinder gasoline engine and ways to predict its behavior in engineering tasks.

Previously, the authors have studied the rotational speed and torque of internal combustion engines for measurement parameters, diagnostics, and improving engine design. This data allowed for the discovery of chaotic behavior in rotational speed. The objective of experimentally tracking the rotational speed was to achieve high resolution and accuracy in time measurement, thereby minimizing rounding and other errors. The data collected were measured with exceptional precision: the rotational speed was recorded at discrete intervals of 0.36 degrees, and time was measured with a precision of 41 nanoseconds. The authors anticipated a random distribution of rotational speed data; however, some graphs revealed unexpected deterministic zones that resembled deterministic chaotic series. Consequently, the goal is to investigate the chaotic nature of the crankshaft speed distribution in internal combustion engines.

2. MATERIALS AND METHODS

Chaos can manifest itself in both continuous (i.e., with dynamics defined by differential equations) and discrete (i.e., with dynamics defined by an iterated map) nonlinear dynamical systems. One of the simplest examples is the logistic map, a one-dimensional, discrete equation that produces chaos at certain growth rates [1]. However, the authors aim to identify a model from experimental data and prove chaotic behavior.

Experimental data were collected from a ZAZ-1103 "Slavuta" vehicle with a MEMZ-2457 motor. To ensure correct measurements, an encoder (HEDS-9040 module and the HEDS-6140#B13 code wheel, Table 1) from AVAGO Technologies with extra high resolution was used (1000 imp/rotation). Normally, encoders within 100 impulses per rotation (sometimes up to 300) are used to track rotational speed and crankshaft position. To ensure sufficient accuracy in measuring time intervals, a quartz resonator of 24.576 MHz was used, which provided a maximum error value of 0.38% at a motor rotation frequency of 5600 rpm [7].

Tab. 1

Characteristics of the HEDS-9040 module
and the code wheel HEDS-6140#B13 from AVAGO Technologies

Parameter	HEDS-9040	HEDS-6140#B13
Operating temperature range	-40°C to +100°C	-40°C to +100°C
Resolution	-	1000 imp/rev
Number of channels	3	3
Maximum rotation frequency	-	30,000 rpm
Permissible shaft axial play	±0.25 mm	±0.25 mm
Permissible eccentricity with radial play not more than	0.1 mm	±0.1 mm
Maximum angular acceleration	250,000 rad/s ²	250,000 rad/s ²
Maximum error per one cycle of a discrete (%) per revolution	5.5° (1.5 x 10 ⁻³ %)	7.5° (2.1 x 10 ⁻³ %)
Maximum shaft position error per revolution	40' (0.19%)	20' (0.09%)

Experiments were conducted on the road with idle regimes at different rotational speeds and with a fully loaded engine moving up a slope. The sensor was located closest to the 4th cylinder, so to avoid the influence of angular oscillations of the crankshaft, differences in sparking, fuel mixing, compression ratios in different cylinders, etc., we tracked cycle-to-cycle series of operation for only the 4th cylinder during only power stroke (180 deg) [8].

In order to analyze the chaotic behavior of the rotational speed of internal combustion engines, a comprehensive approach involving both qualitative and quantitative methods is necessary. The following sections describe the data analysis model employed in this study, incorporating various mathematical techniques and chaos theory principles.

2.1 Data Preprocessing

The first step in the data analysis process is to preprocess the collected experimental data. This involves:

- **Filtering and Smoothing:** Noise in the data is reduced using digital filtering techniques, such as the Savitzky-Golay filter, which smoothens the data while preserving essential features like peak values and overall trends.
- **Normalization:** The data is normalized to remove any biases due to variations in the measurement units or scales.
- **Time Series Construction:** The rotational speed data is converted into a time series format, where each data point represents the engine's speed at a specific time interval.

2.2 Phase Space Reconstruction

Phase space reconstruction is a crucial step in understanding the dynamics of a chaotic system. Takens' theorem provides a framework for reconstructing the phase space from a single time series [9]. The process involves the following steps:

- **Delay Embedding:** Create a delay coordinate matrix from the time series data. The delay embedding method constructs vectors from the time series $x(t)$ as follows:

$$x(t)=[x(t),x(t+\tau),x(t+2\tau),\dots,x(t+(m-1)\tau)] \quad (1)$$

where τ is the time delay and m is the embedding dimension.

- **Selection of Parameters:** The optimal time delay τ and embedding dimension m are determined using methods like the Average Mutual Information (AMI) for τ and the False Nearest Neighbors (FNN) algorithm for m [10].

2.3 Nonlinear Time Series Analysis

Once the phase space is reconstructed, various nonlinear time series analysis techniques are applied to quantify the chaotic behavior:

- **Lyapunov Exponents:** These exponents measure the average rate of separation of infinitesimally close trajectories in the phase space. A positive largest Lyapunov exponent is a strong indicator of chaos. The exponents are calculated using algorithms such as the Wolf algorithm or the Rosenstein method [11].
- **Correlation Dimension:** The correlation dimension D_2 provides a measure of the fractal geometry of the attractor. It is calculated using the Grassberger-Procaccia algorithm,

which involves estimating the scaling behavior of the correlation sum $C(r)$ as a function of the radius r [12]: $C(r) \propto r^{D2}$

- Poincaré Sections: A Poincaré section is a lower-dimensional representation of the system's dynamics. By examining the intersections of trajectories with a chosen plane, one can visualize the structure of the attractor and detect chaotic behavior.

2.4 Statistical Analysis

In addition to nonlinear analysis, statistical methods are used to further characterize the rotational speed data:

- Probability Density Functions (PDFs): The PDFs of the rotational speed are computed to understand the distribution and identify any anomalies or deterministic zones.
- Autocorrelation Functions: The autocorrelation function $R(\tau)$ measures the correlation between the time series and its lagged version. A rapidly decaying autocorrelation function suggests chaotic behavior [10].
- Power Spectral Density (PSD): The PSD analysis helps identify dominant frequencies and the presence of broad-spectrum noise, indicative of chaotic dynamics.

2.5 Surrogate Data Testing

To validate the presence of chaos, surrogate data testing is employed. This involves generating surrogate data sets that preserve some properties of the original data (e.g., amplitude distribution) but are otherwise random. Statistical tests compare the original data with the surrogates to determine if the observed features are genuinely due to chaos or random processes [13].

3. DISCUSSION OF THE RESULTS OF THE EXPERIMENT

We started to analyze data for idle mode with minimal stable rotational speed. Data analysis done by Python with graphic user interface, mathematical/statistical libraries and large language models (numpy, pandas, scipy, matplotlib, sklearn) [13-19]. Data analysis was split into 2 part to increase stability and speed of calculations. All datasets and codes will be able to be downloaded by link [14].

The nature of the rotation of internal combustion engine data is periodic, so normalization should include this. It is because we track “power stroke” of the 4th engine's cylinder and skip for next 540 deg of the crankshaft rotational for the 4th cylinder [8]. By nature of combustion, rotational speed changing impulsivity, so normalized graph like from mean value don't give clear visualization of chaotic distribution due to periodic functionality changing rotational speed with big enough amplitude.

So, to clearly see the chaotic distribution of rotational speed, the normalization of the graph thru periodic function $a \cdot \sin(b \cdot x - c) + d$ (Figure 1 a)-f) should be made.

The graphs a)-d) shows idle with a) ≈ 550 rpm, b) ≈ 1010 rpm, c) ≈ 2160 rpm, d) ≈ 3200 rpm rotational speed accordingly. The graphs e), f) show full gas regime during moving up in the slope 12% and 10% incline, respectively.

Normalized RPM data plot for the same regimes shown in the figure 2 a)-f). Normalization scales the data to have a mean of $a \cdot \sin(b \cdot x - c) + d$ function, making it easier to compare and analyze.

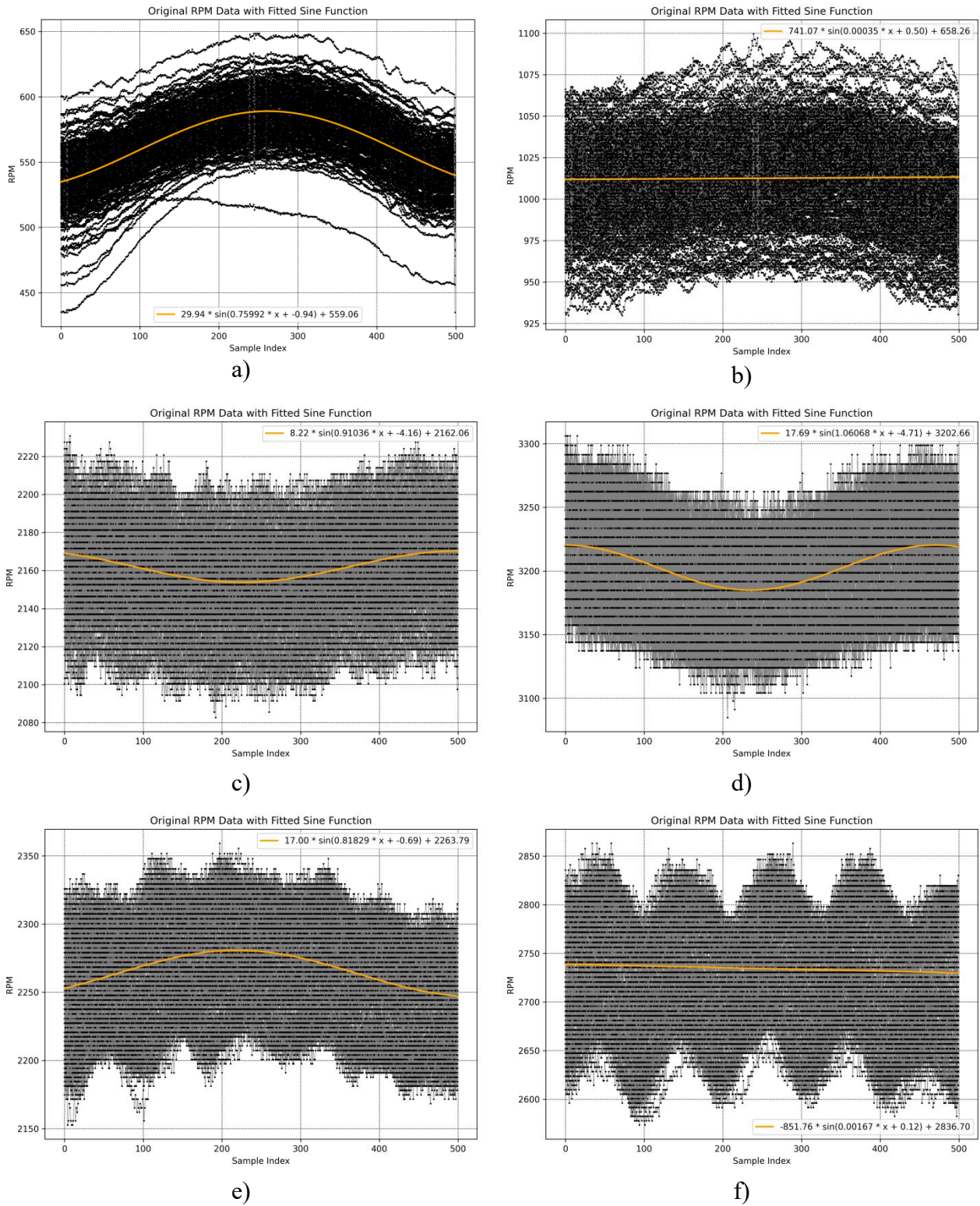


Fig. 1. Rotational Speed Data (Revolutions Per Minute) RPM with approximation at different modes: idle a) ≈ 550 rpm, b) ≈ 1010 rpm, c) ≈ 2160 rpm, d) ≈ 3200 rpm, full gas slope 12%, e) ≈ 2250 rpm, full gas slope 10%, f) ≈ 2740 rpm

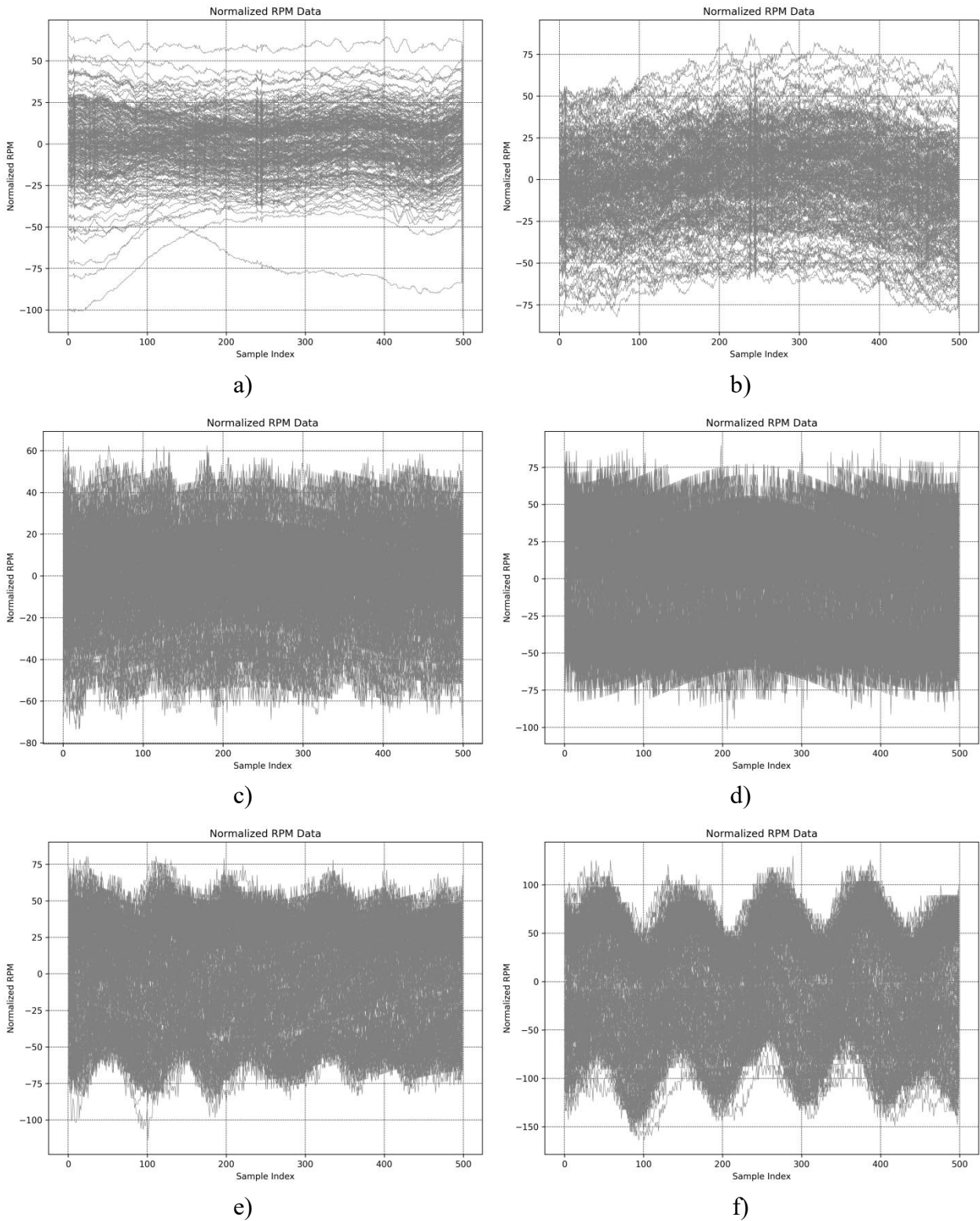


Fig. 2. The normalized RPM data over the sample index: idle a) ≈ 550 rpm, b) ≈ 1010 rpm, c) ≈ 2160 rpm, d) ≈ 3200 rpm, full gas slope 12%, e) ≈ 2250 rpm, full gas slope 10%, f) ≈ 2740 rpm

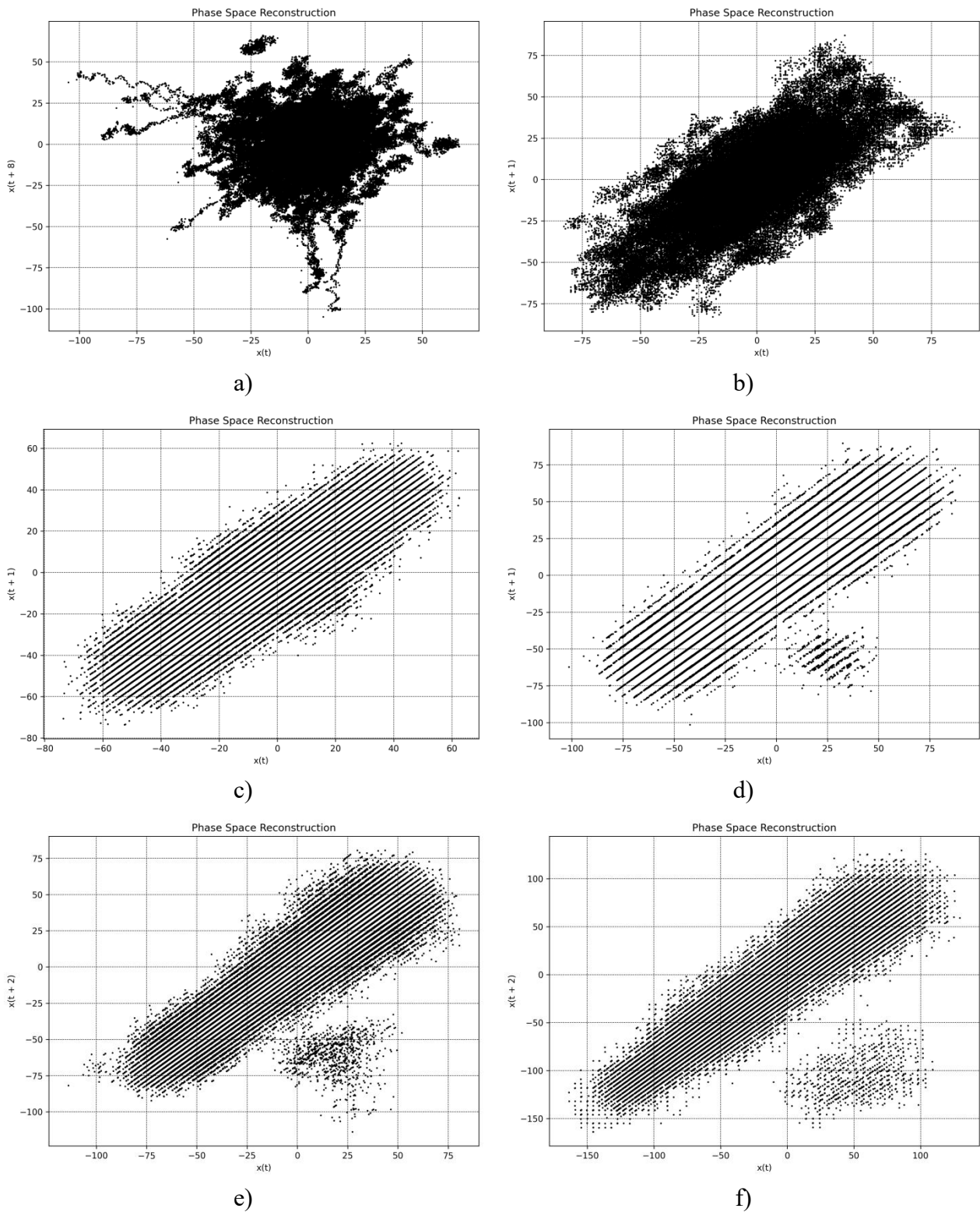


Fig. 3. Phase Space Reconstruction: idle a) ≈ 550 rpm, b) ≈ 1010 rpm, c) ≈ 2160 rpm, d) ≈ 3200 rpm, full gas slope 12%, e) ≈ 2250 rpm, full gas slope 10%, f) ≈ 2740 rpm

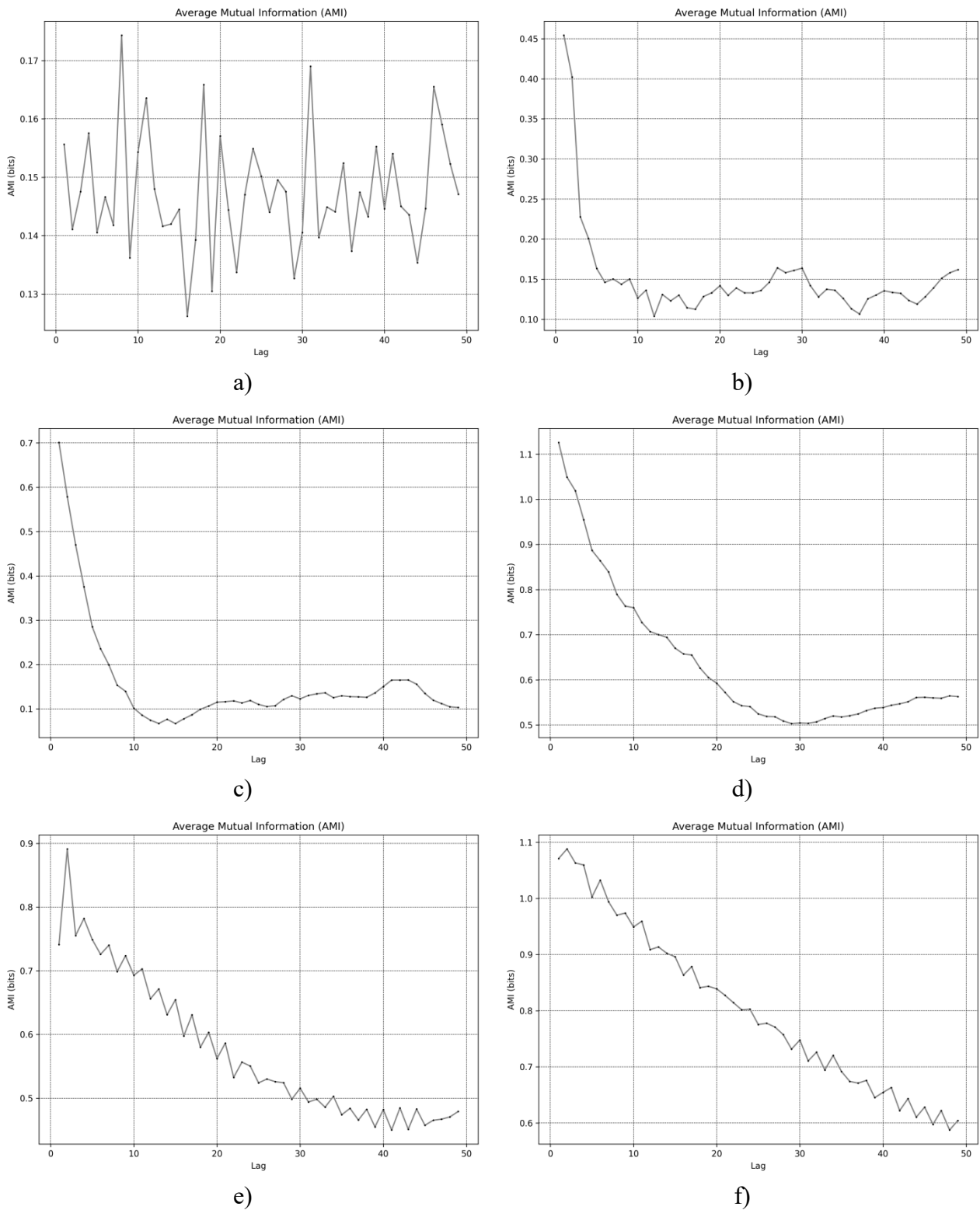


Fig. 4. Average Mutual Information (AMI): idle a) ≈ 550 rpm, b) ≈ 1010 rpm, c) ≈ 2160 rpm, d) ≈ 3200 rpm, full gas slope 12%, e) ≈ 2250 rpm, full gas slope 10%, f) ≈ 2740 rpm

Figures 1 and 2 present the rotational speed data and the normalized RPM, respectively. The raw data exhibits substantial variability, making it challenging to discern clear trends. Normalizing the RPM allows for a more straightforward comparison across different regimes (a-f), but the overall probability distribution remains obscure at first glance. To address this, we employ phase space reconstruction as illustrated in Figure 3.

Figure 4 shows Average Mutual Information (AMI), measures the amount of information shared between the time series and its lagged version as a function of lag. This is crucial for identifying dependencies over time and helps in determining the optimal time delay (τ) for reconstructing the phase space. The first minimum of AMI indicates the lag at which the shared information is least, suggesting the most independent state, and is used to set the optimal time delay for further analysis. For dataset a) the optimal τ is 8. This indicates that the time series shares the least information with its lagged version at a lag of 8, suggesting this as the ideal time delay for phase space reconstruction. For dataset b) the optimal τ is 4. A shorter time delay implies that the system's dynamics change more rapidly compared to dataset a). For dataset c) similar to dataset a), the optimal τ is 8. For dataset d) the optimal τ is 4, indicating rapid changes in system dynamics similar to dataset b). For dataset e) the optimal τ is 5, falling between the time delays observed in datasets a), b), c), and d). The dataset's f) optimal τ is 3, suggesting very rapid changes in the system dynamics.

Figure 5 shows the Sample Entropy for different embedding dimensions (m), quantifying the complexity or irregularity of the time series data. Higher Sample Entropy values indicate greater complexity and unpredictability. By examining the Sample Entropy for varying dimensions, we can identify the optimal embedding dimension for each dataset, which captures the system's dynamics most effectively without over-embedding. It shows Sample Entropy quantifies the complexity or irregularity of the time series data. The optimal embedding dimension (m) is found to be a) $m=10$, b) $m=4$, c) $m=10$, d) $m=4$, e) $m=5$, f) $m=3$. The optimal embedding dimension is crucial for phase space reconstruction, as it ensures that the reconstructed state space retains the essential characteristics of the system's dynamics while minimizing redundancy.

Figure 6 presents the correlation dimension (D_2) for different data chunks. The correlation dimension provides insights into the fractal nature of the data, indicating the system's complexity. Higher values of the correlation dimension suggest more complex and higher-dimensional structures within the time series data. These values indicate varying degrees of complexity across the different datasets, with Dataset b) exhibiting significantly higher correlation dimensions, suggesting a more complex structure.

Figure 7 presents the Probability Density Function (PDF) of the normalized RPM data for datasets a) to f). The PDF provides insights into the distribution of RPM values, with peaks indicating the most frequently observed values. These peaks suggest the dominant operating ranges of the RPM, highlighting where the system tends to operate most frequently.

- Dataset a): Notable peaks around [-55.90, -50.46, -45.02, -31.41, -25.97, -20.53, -12.37, -4.20, 6.68, 12.12, 20.29, 28.45]
- Dataset b): Significant peaks around [-64.23, -57.43, -47.22, -40.42, -33.62, -26.82, -23.42, -20.02, -6.42, 3.78, 13.98, 27.58, 34.38, 41.18]
- Dataset c): Major peaks around [-55.90, -50.46, -45.02, -31.41, -25.97, -20.53, -12.37, -4.20, 6.68, 12.12, 20.29, 28.45]
- Dataset d): Distinct peaks around [-76.59, -68.94, -61.30, -49.83, -42.19, -34.54, -26.89, -19.25, -15.43, -3.96, 7.51, 18.98, 22.80, 34.27, 41.91, 45.74, 57.21]
- Dataset e): Prominent peaks around [-57.48, -49.70, -41.93, -34.15, -25.97, -18.60, -10.83, -6.94, 0.83, 8.61, 16.38, 20.27, 28.05, 31.93, 39.71, 51.37, 55.26, 63.03, 70.81]

- Dataset f): Clear peaks around [-125.68, -119.81, -113.95, -90.48, -72.89, -67.02, -49.42, -31.83, -25.96, -20.10, 3.37, 15.10, 26.83, 38.56, 44.42, 50.29, 56.16, 62.02, 67.89, 79.62, 85.48]

These PDFs (Fig.7) indicate the operational behavior and dominant RPM ranges of the system, providing valuable insights into the system's performance and stability.

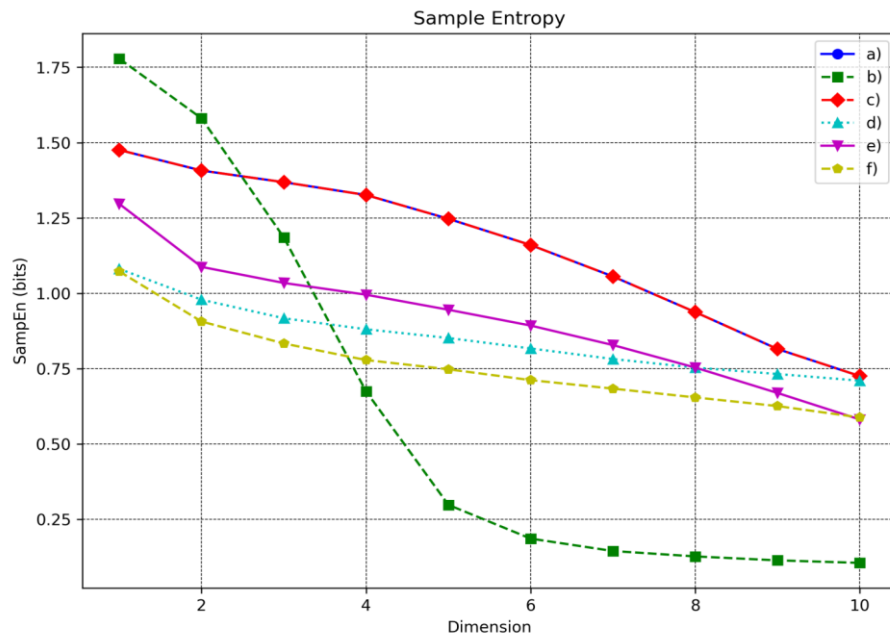


Fig. 5. Sample Entropy (SampEn) : idle a) ≈ 550 rpm, b) ≈ 1010 rpm, c) ≈ 2160 rpm, d) ≈ 3200 rpm, full gas slope 12%, e) ≈ 2250 rpm, full gas slope 10%, f) ≈ 2740 rpm

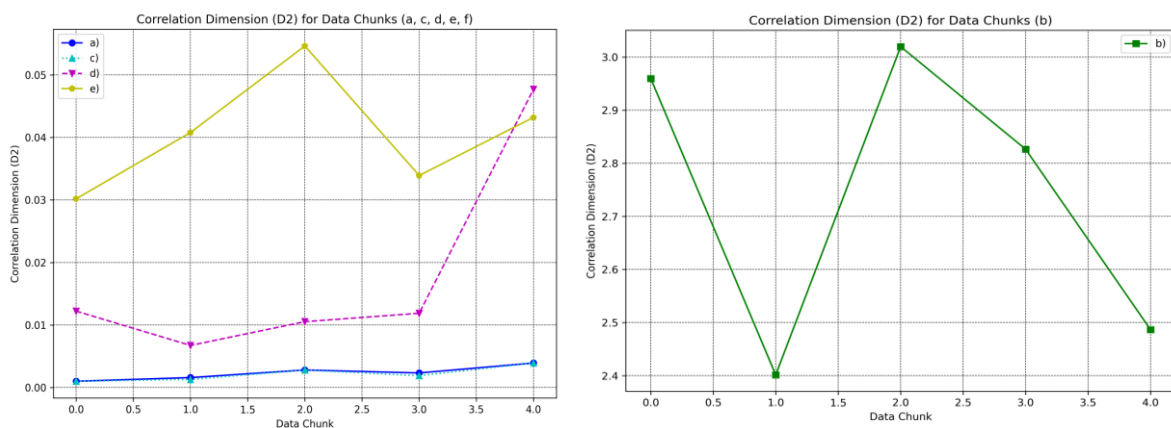


Fig. 6. Correlation dimension (D2) for different data chunks: idle a) ≈ 550 rpm, b) ≈ 1010 rpm, c) ≈ 2160 rpm, d) ≈ 3200 rpm, full gas slope 12%, e) ≈ 2250 rpm, full gas slope 10%, f) ≈ 2740 rpm

Figure 8 presents the Autocorrelation Function (ACF) for different datasets (a) to f)). The ACF measures the correlation of the time series with its lagged versions. The decaying pattern observed in the ACF plots indicates the memory effect in the RPM data, showing how past values influence future values over time.

Dataset a): The ACF shows a gradual decay, indicating a long memory effect, where past values significantly influence future values for a long duration.

Dataset b): The ACF shows a faster decay, suggesting a shorter memory effect, with past values having less influence over a shorter duration.

Dataset c): Similar to dataset a), the ACF shows a gradual decay, indicating a long memory effect.

Dataset d): The ACF shows a moderate decay, suggesting a moderate memory effect with a balanced influence of past values on future values.

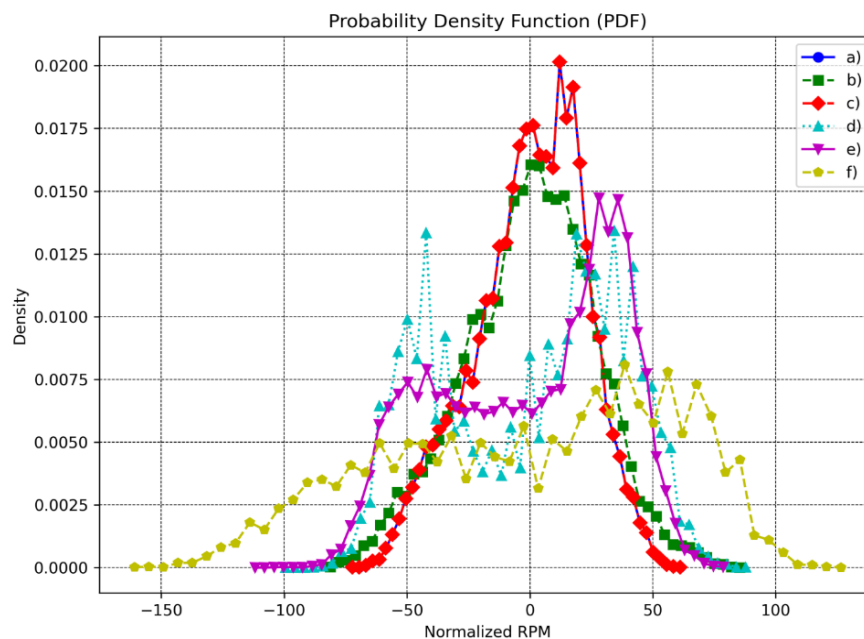


Fig. 7. Shows Probability Density Function (PDF): idle a) ≈ 550 rpm, b) ≈ 1010 rpm, c) ≈ 2160 rpm, d) ≈ 3200 rpm, full gas slope 12%, e) ≈ 2250 rpm; full gas slope 10%, f) ≈ 2740 rpm

Dataset e): The ACF shows a noticeable decay pattern, indicating a significant memory effect, though not as long as datasets a) and c).

Dataset f): The ACF shows a rapid decay, suggesting a very short memory effect, where past values have minimal influence on future values.

Figure 9 presents the Power Spectral Density (PSD) of the normalized RPM data across datasets a) to f). The PSD plot offers a detailed view into the frequency domain characteristics of the RPM data, elucidating how power is distributed across various frequency components.

High Power at Low Frequencies: The PSD reveals a higher concentration of power at low frequencies across all datasets, suggesting that low-frequency components are predominant in the RPM signal. This behavior indicates the presence of slow, large-scale variations within the system's dynamics, which could be linked to underlying processes or external influences that drive such fluctuations.

Decay of Power with Frequency: A noticeable trend in the PSD is the general decay of power as frequency increases. This pattern implies that high-frequency components possess less energy and are consequently less influential in the overall behavior of the RPM data. This decay is typical in systems where high-frequency noise or rapid fluctuations are less dominant.

Distinct Peaks: The PSD plots exhibit distinct peaks at certain frequencies, signifying specific points where the system oscillates more intensely. These peaks are indicative of resonant frequencies or harmonics, where the system's natural frequencies align, resulting in amplified oscillations. Identifying these peaks is crucial for understanding the resonant behavior and potential instabilities within the system.

Comparative Analysis of Datasets: Each dataset demonstrates a unique PSD profile, reflecting the variability in their underlying dynamics. While some datasets show pronounced peaks at certain frequencies, indicating stronger oscillatory behavior, others may exhibit a more uniform distribution of power, suggesting different operating conditions or external influences. Comparing these profiles allows for a deeper understanding of how different conditions or regimes affect the system's frequency response.

The PSD analysis thus provides critical insights into the oscillatory behavior and frequency characteristics of the RPM data. By understanding how power is distributed across frequencies, one can infer the system's stability, identify dominant operational frequencies, and detect potential resonances that could impact performance. This frequency domain perspective complements time-domain analyses, offering a more comprehensive understanding of the system's behavior.

Figure 10 presents the Largest Lyapunov Exponent (LE) calculated for different data chunks across datasets a) to f). The Lyapunov exponent is a critical measure for identifying chaotic behavior within a system, where a positive LE indicates chaos, and a zero or negative LE suggests stable or periodic dynamics. The following parameters were used for the calculations:

Embedding dimension: 3

Time delay: 1`

Minimum time separation: 2

Analysis by dataset:

a) The LE values range from 0.021 to 0.023, indicating significant chaotic behavior. The system shows strong sensitivity to initial conditions, suggesting a highly dynamic and unpredictable RPM behavior in this dataset.

b) The LE values range from 0.003 to 0.007, indicating mild chaotic behavior. While still positive, these lower LE values suggest a system with less pronounced chaos compared to dataset a), but still exhibiting sensitivity to initial conditions.

c) The LE values range from 0.021 to 0.024, very similar to dataset a). This indicates significant chaotic behavior and strong sensitivity to initial conditions, suggesting highly dynamic and unpredictable RPM behavior.

d) The LE values range from -0.004 to 0.014, showing the widest variation among the datasets. This indicates intermittent chaos, where some regions show strong chaotic behavior (positive LE up to 0.014) while others display stable or potentially periodic behavior (negative LE down to -0.004). This dataset suggests complex, varying dynamics in the RPM behavior.

e) The LE values range from 0.004 to 0.008, indicating consistent mild to moderate chaotic behavior. All values are positive, suggesting that the system is consistently sensitive to initial conditions, but with less intensity than datasets a) and c).

f) The LE values range from -0.003 to 0.01, showing significant variation similar to dataset d). This indicates intermittent chaos, with some data chunks showing stable or potentially periodic behavior (negative LE) and others displaying more pronounced chaotic characteristics (positive LE up to 0.01).

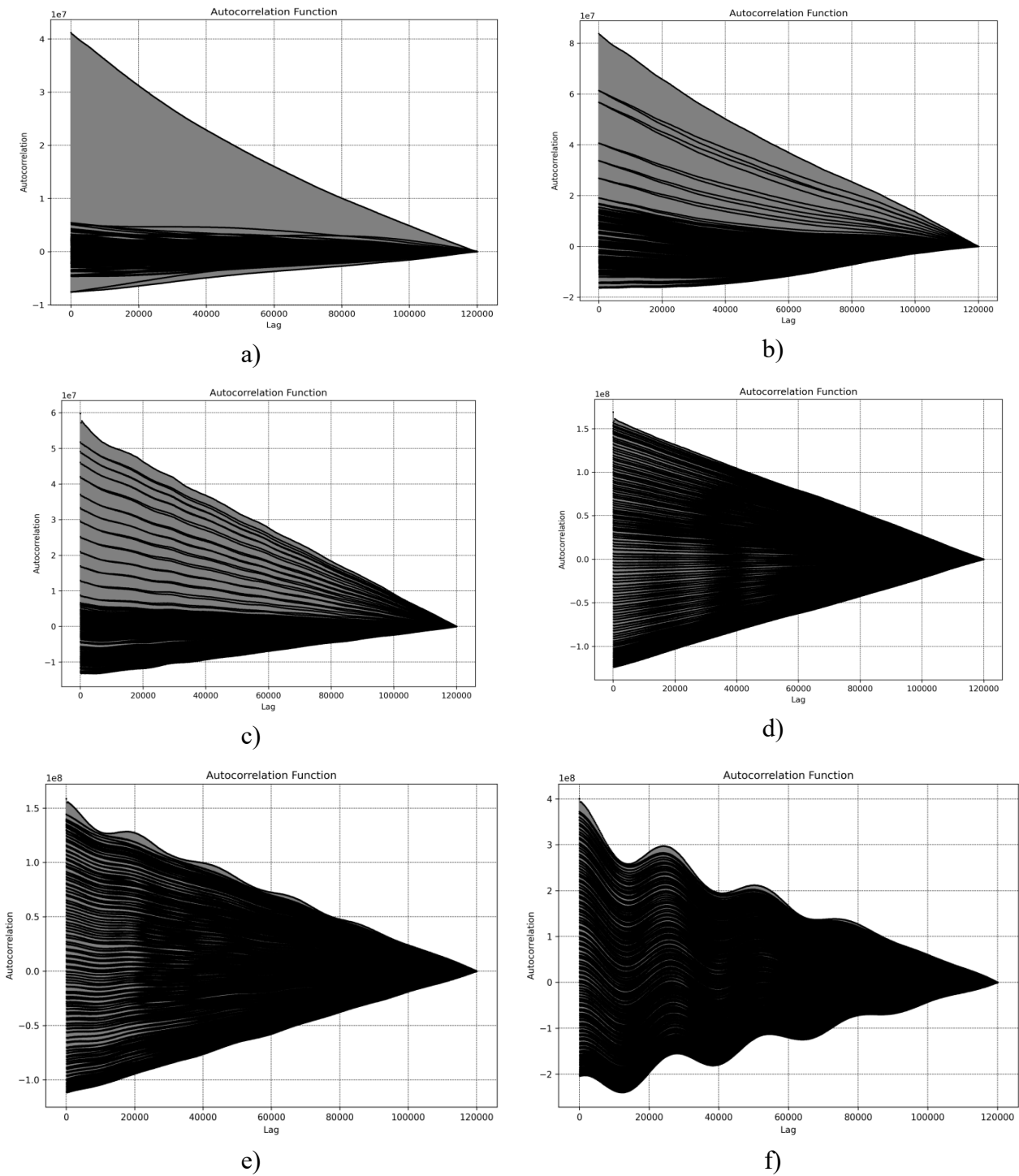


Fig. 8. Autocorrelation Function (ACF): idle a) ≈ 550 rpm, b) ≈ 1010 rpm, c) ≈ 2160 rpm, d) ≈ 3200 rpm, full gas slope 12%, e) ≈ 2250 rpm, full gas slope 10%, f) ≈ 2740 rpm

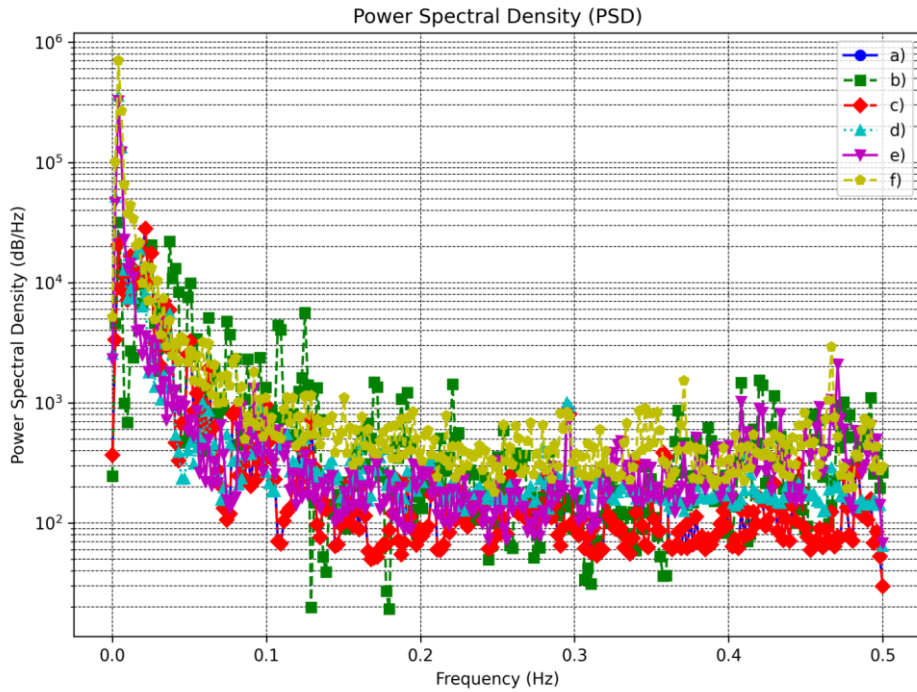


Fig. 9. Power Spectral Density (PSD): idle a) ≈ 550 rpm, b) ≈ 1010 rpm, c) ≈ 2160 rpm, d) ≈ 3200 rpm, full gas slope 12%, e) ≈ 2250 rpm, full gas slope 10%, f) ≈ 2740 rpm

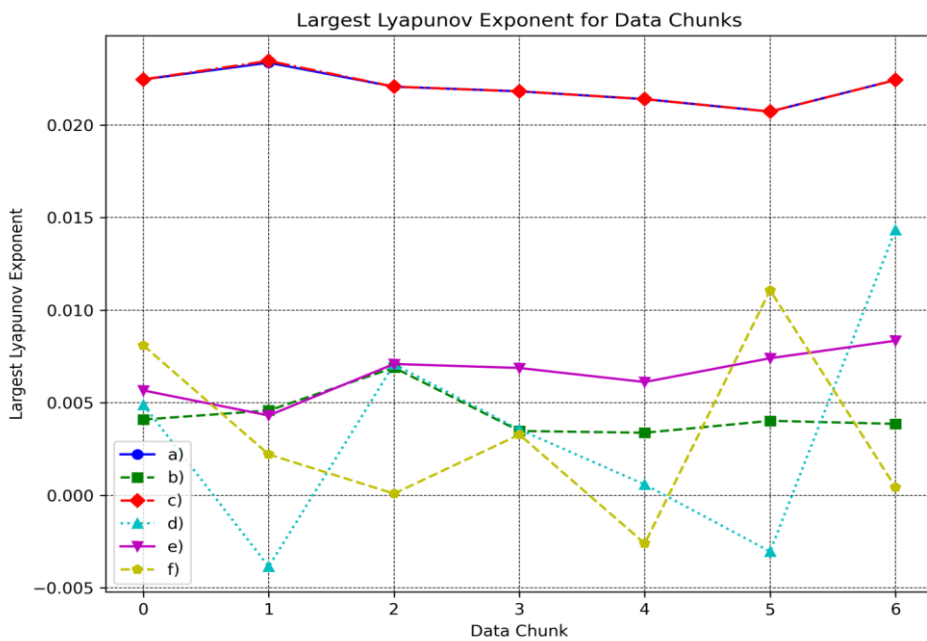


Fig. 10. Lyapunov exponent chunk: idle a) ≈ 550 rpm, b) ≈ 1010 rpm, c) ≈ 2160 rpm, d) ≈ 3200 rpm, full gas slope 12%, e) ≈ 2250 rpm, full gas slope 10%, f) ≈ 2740 rpm

The analysis of Lyapunov exponents provides valuable insights into the system's stability and predictability, highlighting regions where chaotic behavior may impact the RPM's performance. The varying degrees of chaos across different datasets suggest that the internal combustion engine's RPM behavior is highly dependent on specific operating conditions or parameters.

Datasets a) and c) show the most pronounced chaotic behavior, while datasets b) and e) display milder, but consistent chaos. Datasets d) and f) exhibit the most complex dynamics, with intermittent chaos and periods of stability or potential periodicity.

This comprehensive analysis across all datasets reveals a rich tapestry of dynamic behaviors in the internal combustion engine's RPM, ranging from strongly chaotic to near-stable conditions, depending on the specific dataset and operating parameters.

The analysis of the data presented in Figures 1 through 10 reveals significant evidence of chaotic behavior across various operating conditions. Key findings include:

1. Evidence of Chaos: The Largest Lyapunov Exponent (LE) values consistently show positive values across all datasets, ranging from 0.003 to 0.024. This indicates the presence of chaos in the system, suggesting that the RPM is sensitive to initial conditions and exhibits exponential divergence in trajectories over time.
2. Complexity of the System: The Sample Entropy analysis identified optimal embedding dimensions ranging from 3 to 10 across different datasets. Higher values indicate greater irregularity and unpredictability in the time series data. The correlation dimension values varied significantly, with some datasets showing higher dimensions, suggesting a more complex structure.
3. Optimal Time Delay: The Average Mutual Information (AMI) analysis determined optimal time delays (τ) ranging from 3 to 8 across different datasets. This variation in optimal time delays indicates that the system's dynamics change at different rates under various operating conditions.
4. Memory Effects: The Autocorrelation Function (ACF) analysis revealed varying degrees of memory effects across the datasets. Some regimes exhibited long memory effects, where past values significantly influence future values over an extended period, while others showed short memory effects with rapidly decaying correlations.
5. Frequency Domain Insights: The Power Spectral Density (PSD) analysis showed that low-frequency components dominate the RPM signal across all datasets, indicating slow, large-scale variations in the system. Distinct peaks at certain frequencies suggest the presence of resonant frequencies or harmonics, which are critical for understanding the system's oscillatory behavior and potential instabilities.
6. Varying Chaotic Behavior: The analysis revealed different levels of chaotic behavior across operating conditions:

Datasets a) and c) (idle at ≈ 550 rpm and ≈ 2160 rpm) showed the most pronounced chaotic behavior with LE values ranging from 0.021 to 0.024.

Datasets b) and e) (idle at ≈ 1010 rpm and full gas slope 12% at ≈ 2250 rpm) displayed milder but consistent chaotic behavior.

Datasets d) and f) (idle at ≈ 3200 rpm and full gas slope 10% at ≈ 2740 rpm) exhibited the most complex dynamics, with intermittent chaos and periods of stability or potential periodicity.

Implications for System Monitoring and Control:

1. Challenges in Long-Term Prediction: The chaotic nature of the system makes long-term precise predictions inherently challenging. Small differences in initial conditions can lead to vastly different outcomes over time.

2. Importance of Short-Term Forecasting: While long-term predictions may be unreliable, short-term forecasting can still be valuable. Understanding the system's immediate dynamics can help anticipate short-term changes and inform decision-making.
3. Advanced Control Strategies: The varying degrees of chaos across different operating conditions suggest that adaptive control strategies are necessary. These strategies should account for the system's nonlinear dynamics and be able to adjust to different chaotic regimes.
4. Resonance Management: The PSD analysis revealed distinct peaks at certain frequencies. Managing these resonant frequencies could be crucial for maintaining system stability and optimizing performance.
5. Real-time Monitoring: Given the system's sensitivity to initial conditions and its complex dynamics, real-time monitoring of the RPM becomes essential for detecting and responding to potential instabilities or performance issues.

4. DISCUSSION

The analysis, employing various techniques from chaos theory and nonlinear dynamics, provides a detailed picture of the engine's behavior under various operating conditions. Results show that RPM dynamics exhibit different levels of chaos and complexity depending on the engine's operating regime, with implications for engine design, control, and diagnostics.

To facilitate further research and collaboration, the authors have shared the original datasets and analyzed Python code [15]. This openness allows for verification of results, further exploration of complex processes in internal combustion engines, and investigation into the influence of chaotic dynamics versus random fluctuations on engine behavior.

The authors welcome further discussion and collaboration to deepen our understanding of these complex dynamics and their implications for engine performance, efficiency, and control strategies. This study builds upon previous work in the field and extends the application of chaos theory to the analysis of RPM fluctuations, providing a comprehensive framework for analyzing engine dynamics that could be applied to various engine types and operating conditions.

By combining high-precision measurements with advanced analytical techniques, this research opens new avenues for understanding and optimizing internal combustion engine performance, highlighting the importance of considering nonlinear and chaotic behaviors in engine analysis and design.

5. CONCLUSIONS

The analysis of the rotational speed data reveals significant chaotic behavior in the internal combustion engine's RPM across various operating conditions:

1. Lyapunov Exponents: highest 0.024 (idle at ≈ 550 rpm and ≈ 2160 rpm), indicating strong chaos and high sensitivity to initial conditions; lowest: -0.004 (idle at ≈ 3200 rpm), suggesting occasional periods of stability. The predominantly positive Lyapunov Exponents confirm the presence of chaos in the system.
2. Optimal Time Delay (τ): ranges from 3 to 8 across datasets, shortest ($\tau = 3$) at full gas, slope 10%, ≈ 2740 rpm, indicating rapid changes in system dynamics, longest ($\tau = 8$) at idle, ≈ 550 rpm and ≈ 2160 rpm, suggesting slower changes in system dynamics.

3. Optimal Embedding Dimension (m): ranges from 3 to 10 across datasets, highest (m = 10) at idle, ≈ 550 rpm and ≈ 2160 rpm, suggesting high system complexity, lowest (m = 3) at full gas, slope 10%, ≈ 2740 rpm, indicating simpler system dynamics.
4. Power Spectral Density: all datasets show higher concentration of power at low frequencies (0.1 Hz to 0.5 Hz), indicating dominance of slow, large-scale fluctuations.

References

1. Boeing Geoff. 2016. "Visual analysis of nonlinear dynamical systems: chaos, fractals, self-similarity and the limits of prediction". *Systems* 4: 37. DOI: 10.3390/systems4040037.
2. Stewart Ian. 2000. "The lorenz attractor exists". *Nature* 406: 948-949. DOI: 10.1038/35023206.
3. Wendeker Mirosław, Jacek Czarnigowski, Grzegorz Litak, Kazimierz Szabelski. 2003. "Chaotic Combustion in spark ignition engines". *Chaos Solitons & Fractals* 18(4): 803-806. DOI: 10.1016/S0960-0779(03)00031-6.
4. Huanyu Di, Shen Tielong. 2018. "Experimental analysis of chaotic property of in-cylinder combustion of si engine." *37th Chinese Control Conference (CCC)*: 7907-7911. Wuhan, China. DOI: 10.23919/ChiCC.2018.8483466.
5. Lima, Thyago L. de V., Abel C.L. Filho, Francisco A. Belo, Filipe V. Souto, Thaís C.B. Silva, Koje V. Mishina, Marcelo C. Rodrigues. 2021. "Noninvasive methods for fault detection and isolation in internal combustion engines based on chaos analysis". *Sensors* 21(20): 6925. DOI: 10.3390/s21206925.
6. Grabar Ivan, Andrii Ivanchenko, Volodymyr Lomakin, Dmytro Kalinkin, Oleksandr Kuharchuk. 2010. "Hardware and software complex for analyzing the operation of the MeMZ-2457 engine by rotation frequency fluctuation". *Scientific Notes of the National Technical University* 28: 151-156.
7. Lomakin Volodymyr. 2018. "Decreasing of speed fluctuation of internal combustion engine by improving the flywheel design". *Doctoral dissertation*. Available at: http://diser.ntu.edu.ua/Lomakin_dis.pdf.
8. Takens Floris. 1981. "Detecting strange attractors in turbulence". *Dynamical Systems and Turbulence* 898: 366-381.
9. Holger Kantz, Thomas Schreiber. 2004. *Nonlinear time series analysis*. Cambridge University Press.
10. Wolf Alan, Jack B. Swift, Harry L. Swinney, John A. Vastano. 1985. "Determining Lyapunov exponents from a time series". *Physica D: Nonlinear Phenomena* 16(3): 285-317. DOI: 10.1016/0167-2789(85)90011-9.
11. Grassberger Peter, Itamar Procaccia. 1983. "Measuring the strangeness of strange attractors". *Physica D: Nonlinear Phenomena* 9(1-2): 189-208. DOI: 10.1016/0167-2789(83)90298-1.
12. Theiler James, Stephen Eubank, André Longtin, Bryan Galdrikian, J. Doyne Farmer. 1992. "Testing for nonlinearity in time series: the method of surrogate data". *Physica D: Nonlinear Phenomena* 58(1-4): 77-94. DOI: 10.1016/0167-2789(92)90102-S.
13. *Chaotic-engine-rpm-analysis project with raw data*. Available at: <https://github.com/VD45/chaotic-engine-rpm-analysis>.

14. *Numpy 2.0*. The fundamental package for scientific computing with Python. Available at: <https://numpy.org/>.
15. *Pandas*. The fast, powerful, flexible and easy to use open source data analysis and manipulation tool, built on top of the Python programming language. Available at: <https://pandas.pydata.org/>.
16. *SciPy*. Fundamental algorithms for scientific computing in Python. Available at: <https://scipy.org/>.
17. *Matplotlib*. Visualization with Python. Available at: <https://matplotlib.org/>.
18. *SciKit*. Machine Learning in Python. Available at: <https://scikit-learn.org/stable/>.
19. Python Programming Language. Available at: <https://www.python.org/>.

Received 10.01.2025; accepted in revised form 05.04.2025



Scientific Journal of Silesian University of Technology. Series Transport is licensed under a Creative Commons Attribution 4.0 International License